Journal of Alloys and Compounds 481 (2009) 568–572

Contents lists available at ScienceDirect

Journal of Alloys and Compounds

journal homepage: www.elsevier.com/locate/jallcom

Preparation, characterization and photoluminescence of nanocrystalline calcium molybdate

Anukorn Phuruangrat[a,*], Titipun Thongtem[b,*], Somchai Thongtem[a]

[a] Department of Physics and Materials Science, Faculty of Science, Chiang Mai University, Chiang Mai 50200, Thailand
[b] Department of Chemistry, Faculty of Science, Chiang Mai University, Chiang Mai 50200, Thailand

ARTICLE INFO

Article history:
Received 1 January 2009
Received in revised form 4 March 2009
Accepted 5 March 2009
Available online 19 March 2009

Keywords:
Nanocrystalline calcium molybdate
Scheelite structure
Microwave radiation

ABSTRACT

Nanocrystalline calcium molybdate was successfully synthesized from $Ca(NO_3)_2$ and Na_2MoO_4 in ethylene glycol using a microwave radiation method. Body-centered tetragonal structured calcium molybdate with narrow nanosized distribution was detected using XRD, SAED and TEM. A diffraction pattern was also simulated and was found to be in accordance with those obtained from the experiment and JCPDS standard. Raman and FTIR spectra show the Mo–O prominent stretching bands in the $[MoO_4]^{2-}$ tetrahedrons at 879.59 and 743–895 cm^{-1}, respectively. Photoluminescence emission of $CaMoO_4$ was detected at 477 nm, caused by the annihilation of a self-trapped excitons from the $[MoO_4]^{2-}$ excited complex.
© 2009 Elsevier B.V. All rights reserved.

1. Introduction

Nanomaterials have very interesting optical and electrical properties which are different from their bulks and controlled by their uniform shapes and narrow size distributions. Alkaline earth metal molybdates are very interesting materials due to their structural properties, and great potential and many promising applications. They have attracted particular interest in a variety of applications, such as laser host materials, luminescence materials, microwave applications, microelectronics and catalysts [1–5]. There are a variety of methods used to synthesize nanosized $CaMoO_4$, such as molten salt [4], a modified citrate complex method using microwave irradiation [5] sonochemical method [6], and pulsed laser ablation [7].

In recent years, microwave irradiation has been used for a number of applications in preparing materials, including inorganic complexes, oxides, sulfides and others. Microwave irradiation has shown to be very rapid growth in its application to materials science and engineering due to its unique reaction effect, such as rapid volumetric heating and the consequent dramatic increase in reaction rates [8,9]. A solvent with high dielectric constant is very rapidly heated up to high temperature by microwave irradiation at very short time. Ethylene glycol, which has a dielectric constant of 40.3 at 298 K [10], is excellent in coupling with the oscillating electric field intensity, leading to molecular vibration. The solution is able to attain high temperature at very rapid rate. Due to the vibration of a 2.45 GHz microwave radiation [11], nucleation and growth proceeded in uniform liquid phase environment. The microwave radiation has the advantage of short reaction time, simple and efficient over other conventional methods. The products have small particle sizes, narrow particle size distributions and high purity [9].

In 2005, Ryu et al. [5] reported the synthesis of nanosized $CaMoO_4$ powders at low temperatures by a modified citrate complex method using microwave irradiation. The nanosized $CaMoO_4$ powders were produced when the citrate complex precursors were calcined at 500 °C and above for 3 h. For the present research, the characterization and photoluminescence (PL) of nanocrystalline $CaMoO_4$ synthesized by a microwave irradiation method with no calcination are reported.

2. Experimental procedure

To synthesize nanocrystalline $CaMoO_4$, each 0.005 mol of $Ca(NO_3)_2$ and Na_2MoO_4 was separately dissolved in 15.00 ml ethylene glycol. The two solutions were mixed and stirred for 30 min. Then the mixture was transferred into a homemade autoclave and heated at 50% of 600 W microwave for 20 min. For the 50% of 600 W microwave-assisted synthesis, the power was on for 60 s and off for 60 s interval every 120 s $cycle^{-1}$. At the conclusion of the process, white precipitates were produced, separated using a filtered paper, washed with distilled water and absolute ethanol, and dried in air at 80 °C for 24 h. The product was then analyzed by X-ray diffraction (XRD), Fourier transform inferred (FTIR) spectroscopy and Raman spectroscopy, transmission electron microscopy (TEM), selected area electron diffraction (SAED) and a spectrophotometry.

* Corresponding authors. Tel.: +66 0 53 943341–45; fax: +66 0 53 892277.
E-mail addresses: phuruangrat@hotmail.com (A. Phuruangrat), ttpthongtem@yahoo.com (T. Thongtem).

0925-8388/$ – see front matter © 2009 Elsevier B.V. All rights reserved.
doi:10.1016/j.jallcom.2009.03.037

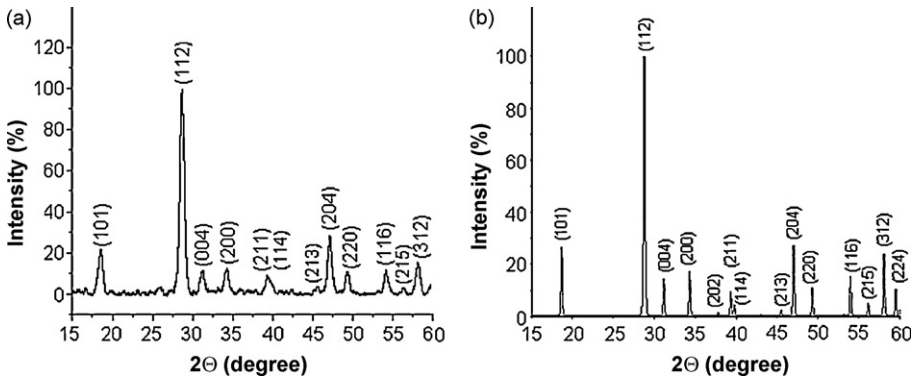

Fig. 1. (a) XRD pattern of $CaMoO_4$ synthesized using a microwave radiation and (b) the simulated diffraction pattern.

3. Results and discussion

Fig. 1a shows the XRD pattern of nanocrystalline $CaMoO_4$, prepared from $Ca(NO_3)_2$ and Na_2MoO_4 by a microwave irradiation method. The pattern was compared to the JCPDS card no. 29-0351 [12] ($a = b = 5.2260$ Å and $c = 11.4300$ Å). All of the diffraction peaks were specified that the product was tetragonal $CaMoO_4$ structure with no detection of any impurities, like MoO_3, CaO, or others. Calculated lattice parameters of the product are $a = b = 5.2178$ Å and $c = 11.4632$ Å, which are very close to those of the corresponding JCPDS card [12].

The crystallite size of nanocrystalline $CaMoO_4$ was calculated using the (1 1 2) peak of the XRD pattern and the Scherrer's equation:

$$B = \frac{\lambda k}{L \cos\theta},$$

where λ is the wavelength of Cu Kα radiation, θ the Bragg's angle, L the average crystallite size, k a constant ($k = 0.89$) and B is the full width at half maximum (FWHM) of the (1 1 2) peak in radian [13], and was found to be 15 nm.

To produce nanocrystalline $CaMoO_4$, $Ca(NO_3)_2$ reacted with Na_2MoO_4 in ethylene glycol under basic condition using a microwave radiation:

$$Ca(NO_3)_2 + Na_2MoO_4 \rightarrow CaMoO_4 + 2NaNO_3$$

Scheelite structured metal molybdates with respective ionic radii of 1.12, 1.25, 1.42 and 1.29 Å for Ca, Sr, Ba and Pb [14] are body-centered tetragonal symmetry C_{4h}^6 at room temperature, and have two formula units per primitive cell [14–16]. Each Mo site is surrounded by four equivalent O sites in tetrahedral symmetry and each divalent metal shares corners with eight adjacent $[MoO_4]^{2-}$ tetrahedrons [1,15,16]. Calcium molybdate with $I4_1/a$ space group [12] was simulated using CaRIne version 3.1 program [17] and its calculated lattice cell. The calcium molybdate unit cell (Fig. 2) shows a complex structure composing of layers normal to the z-axis. Each of them has a two-dimensional cesium chloride type arrangement of Ca^{2+} divalent ion and $[MoO_4]^{2-}$ tetrahedral configuration, which are surrounded by eight ions of opposite sign [15,16,18]. The simulated XRD pattern using CaRIne version 3.1 program [17] and the Cu Kα line (1.5418 Å [9,11]) is shown in Fig. 1b. The 2θ angles and intensities of different peaks obtained from the simulation, experiment, and JCPDS standard [12] is shown in Table 1. It is worth noting that their values are in good accordance, although the (2 0 2) low intensity peak of the JCPDS standard was not detected in the experiment.

Metal molybdates have $[MoO_4]^{2-}$ molecular ionic groups with strong covalent Mo–O bonding, but M^{2+} cations such as Ca, Sr, Ba and Pb are weakly couple with the ionic groups [14]. Their Raman

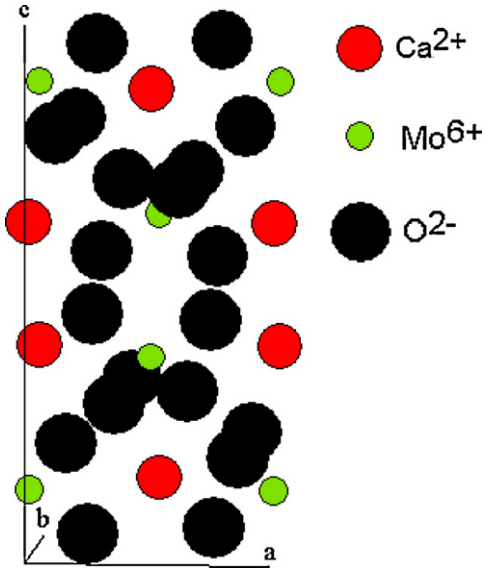

Fig. 2. Unit cell of tetragonal $CaMoO_4$.

vibrations are classified into two types, the internal and external modes. The first is caused by the oscillation inside the $[MoO_4]^{2-}$ molecular ionic groups with immobile mass center. The second is the lattice phonon vibration, due to the motion of M^{2+} cations relative to the rigid molecular ionic units. In free space, $[MoO_4]^{2-}$ ions have T_d-symmetry. By using factor group analysis, it follows that $3N = 15$ degrees of freedom for $[MoO_4]^{2-}$ molecular ionic groups are composed of four internal modes denoted by $v_1(A_1)$, $v_2(E)$, $v_3(F_2)$

Table 1
The 2θ diffraction angles (°) and diffraction intensities of $CaMoO_4$ obtained from the JCPDS card no. 29-0351 [12], experiment and simulation.

Plane	JCPDS 29-0351		Experiment		Simulation	
	2θ	Intensity	2θ	Intensity	2θ	Intensity
(1 0 1)	18.63	25.00	18.44	21.14	18.67	26.40
(1 1 2)	28.78	100.00	28.69	100.00	28.75	100.00
(0 0 4)	31.25	14.00	31.18	11.04	31.18	14.40
(2 0 0)	34.33	16.00	34.34	11.52	34.35	16.90
(2 0 2)	37.82	4.00	–	–	37.86	1.50
(2 1 1)	39.31	10.00	39.27	8.64	39.37	8.30
(1 1 4)	39.82	6.00	40.06	5.62	39.80	4.20
(2 1 3)	45.47	6.00	45.70	3.24	45.51	2.20
(2 0 4)	47.07	30.00	47.12	28.12	47.07	27.40
(2 2 0)	49.27	14.00	49.37	10.58	49.36	10.80
(1 1 6)	54.09	14.00	54.15	11.02	54.00	15.10
(2 1 5)	56.22	6.00	56.16	2.65	56.20	4.90
(3 1 2)	58.04	20.00	58.05	14.39	58.13	23.90

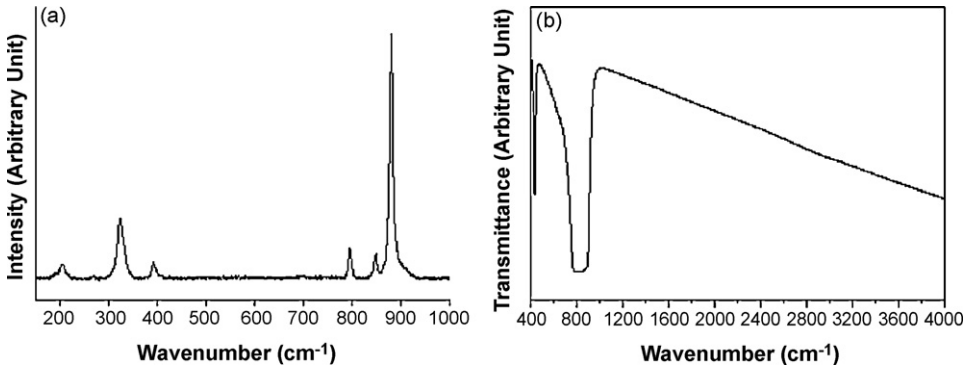

Fig. 3. (a) Raman and (b) FTIR spectra of $CaMoO_4$ synthesized using a microwave radiation.

and $v_4(F_2)$, one free rotation (f.r.) mode (F_1) and one translation mode (F_2). In scheelite body-centered tetragonal structure, its symmetry is reduced to be S_4. All degenerative modes are split, due to the crystal field effect. The split is also caused by two formula units per primitive cell of the scheelite structure, specified as the effect of Davydov splitting. Group theory calculation shows that there are 26 different modes, $\Gamma = 3A_g + 5A_u + 5B_g + 3B_u + 5E_g + 5E_u$, for zero wavevector of the scheelite primitive cell. The $3A_g$, $5B_g$ and $5E_g$ modes are Raman active. Only four of the $5A_u$ and $5E_u$ modes are infrared (IR) active, and their remains are acoustic vibrations. The $3B_u$ modes are silent [14]. $CaMoO_4$ has $[MoO_4]^{2-}$ tetrahedron symmetry. Raman spectrum of $CaMoO_4$ crystals was characterized over 150–1000 cm^{-1} as shown in Fig. 3a. The $v_{f.r.}(A_g)$, $v_2(A_g)$, $v_4(B_g)$, $v_3(E_g)$, $v_3(B_g)$ and $v_1(A_g)$ modes were detected at 203.55, 322.70, 392.38, 795.08, 847.50 and 879.59 cm^{-1}, respectively. The present results correlate well with those previously obtained [19]. Comparing to Ar laser with 514.5 nm wavelength, a great deal of energy was lost during the Raman analysis, due to the inelastic scattering process. In addition, a transmittance mode of $CaMoO_4$ was analyzed by FTIR as shown in Fig. 3b. For T_d-symmetry, the scheelite structure has four vibrations, specified as $v_1(A_1)$, $v_2(E)$, $v_3(F_2)$ and $v_4(F_2)$ [20]. In lattice space, its IR spectrum is in accordance with the S_4 site symmetry. The correlations of the $T_d \leftrightarrow S_4$ symmetries are $A_1 \leftrightarrow A$, $E \leftrightarrow A + B$ and $F_2 \leftrightarrow B + E$. There was no detection of the v_1 mode. Only the v_2, v_3 and v_4 modes were detected [20]. For the present analysis, a strong transmittance mode specified as Mo–O anti-symmetric stretching vibration (v_3) of $[MoO_4]^{2-}$ tetrahedrons [21] was detected at 743–895 cm^{-1}. Additional weak peak of Mo–O bending mode (v_4) [21] was at 423 cm^{-1}. The results are in accordance with those previously reported [22].

TEM image, SAED pattern and particle size distribution of $CaMoO_4$ nanocrystalline are shown in Fig. 4. The product was composed of a number of round nanosized particles. Its SAED pattern shows a number of bright spots arranged in concentric rings, with the calculated lattice planes obtained from the diameters of the diffraction rings. For the present research, the product is polycrystalline in nature. Among the diffraction planes, they are (1 0 1), (1 1 2), (0 0 4), (2 0 0), (1 1 4), (2 0 4), (2 2 0), (1 1 6) and

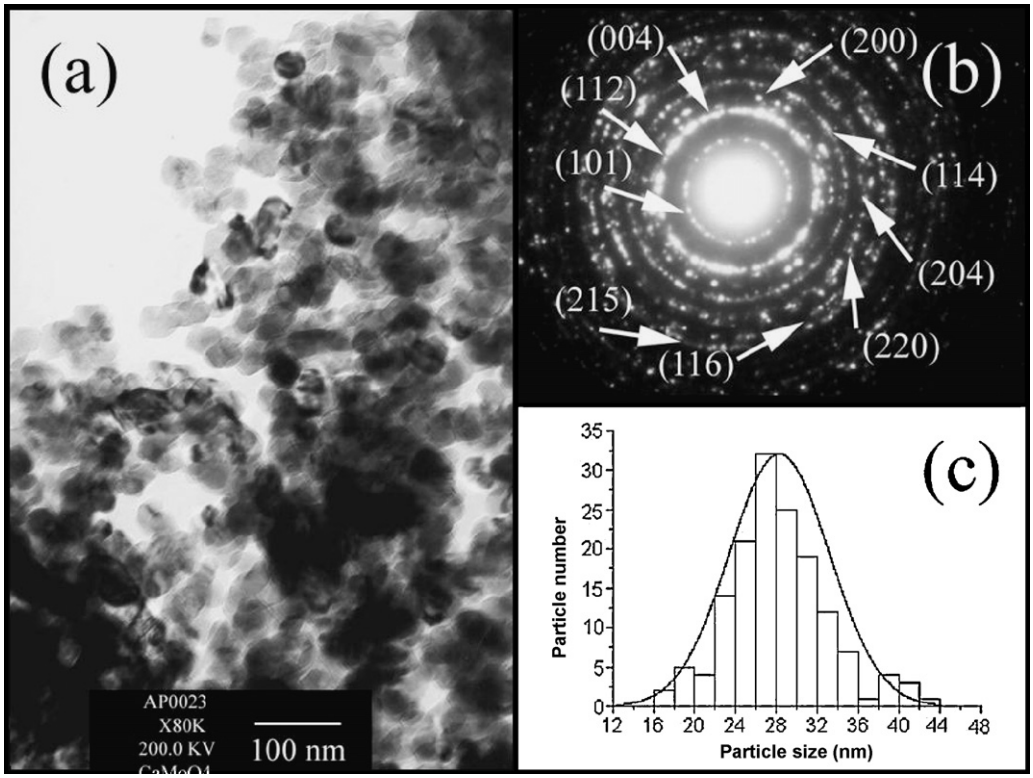

Fig. 4. (a) TEM image, (b) SAED pattern and (c) particle size distribution of $CaMoO_4$ synthesized using a microwave radiation.

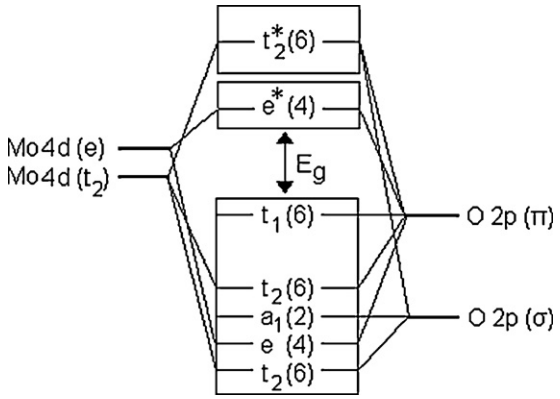

Fig. 5. Schematic diagram of the crystal-field splitting and hybridization of the molecular orbitals of $[MoO_4]^{2-}$ tetrahedrons.

(2 1 5), which are in accordance with those of the JCPDS standard for $CaMoO_4$ [12]. The size distribution was determined from 150 particles of the TEM image. The $CaMoO_4$ nanoparticles have narrow size distribution, and are in favor their luminescent properties. The particle sizes are in the range of 16–44 nm with the average of 28 nm.

To produce $CaMoO_4$ round nanoparticles, $Ca(NO_3)_2$ reacted with Na_2MoO_4 in ethylene glycol under a microwave radiation, and $CaMoO_4$ molecules began to exist. Simultaneously, several of the molecules nucleated to form nuclei. As the time passed, the nuclei grew by the diffusion of nearby molecules to form nanoparticles. Their sizes were limited by the diffusion rate and concentration of the nearby molecules, length of time, microwave power and others, but their round shape was controlled by their isotropic growth in all directions. Some nanoparticles clustered together in groups as well. This is the cause of the difference in the particle sizes obtained by the calculation using Scherrer's equation and the measurement from TEM image.

The emission shape of $CaMoO_4$ nanoparticles may be explained by considering Jahn–Teller splitting effect on the excited states of tetrahedral $[MoO_4]^{2-}$ anions. The crystal-field splitting and hybridization of the molecular orbitals of $[MoO_4]^{2-}$ tetrahedrons are shown in Fig. 5. For the ground state, all one-electron states below the energy band gap (E_g) are filled, resulting in the $^1A_1$ many-electron ground states. At the lowest excited states, there are one-hole in the t_1 states of the valence band and one-electron in the e states of the conduction band, corresponding to the $^1T_1$, $^1T_2$, $^3T_1$ and $^3T_2$ many-electron excited states. Only the electronic transition between $^1T_2$ and $^1A_1$ states is allowed

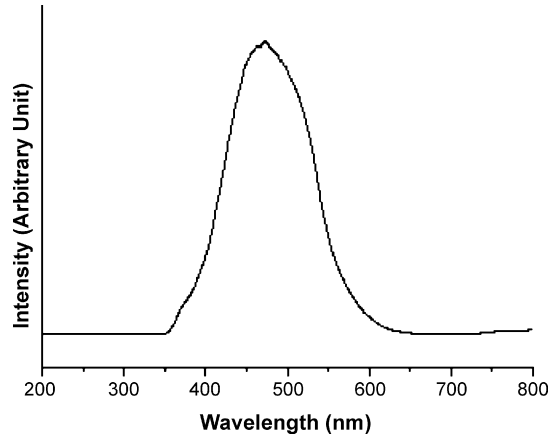

Fig. 6. PL spectrum of $CaMoO_4$ synthesized using a microwave radiation.

[23–25]. The emission is caused by the recombination of electrons in the $^1T_2$ excited state and holes in the $^1A_1$ ground state. Fig. 6 shows photoluminescence of $CaMoO_4$ nanocrystalline using a 212 nm excitation wavelength. It shows the maximum emission peak at 477 nm, specified as the intrinsic emission, and was caused by the annihilation of a self-trapped excitons from the $[MoO_4]^{2-}$ excited complex. It can be excited either in the excitonic absorption band or in the recombination process of the scheelite structured $CaMoO_4$ [26]. At room temperature, the $^3T_1$ and $^3T_2$ excited states are also involved in the intrinsic emission by a spin–forbidden transition to the $^1A_1$ ground state in optically detected electron paramagnetic resonance of $CaMoO_4$. The transition from the triplets at the excited states to the ground state was clearly detected, and was the cause to broaden the PL spectrum [23].

4. Conclusions

$CaMoO_4$ nanocrystallines were successfully produced from $Ca(NO_3)_2$ and Na_2MoO_4 in ethylene glycol by a one step microwave radiation method with no further calcination. The body-centered tetragonal $CaMoO_4$ structure with a narrow particle size distribution of 16–44 nm was detected using XRD, SAED and TEM. The $v_{f.r.}(A_g)$, $v_2(A_g)$, $v_4(B_g)$, $v_3(E_g)$, $v_3(B_g)$ and $v_1(A_g)$ modes were detected using Raman spectroscopy, and very strong Mo–O antisymmetric stretching mode (v_3) in $[MoO_4]^{2-}$ molecular ionic groups using FTIR. The PL intrinsic emission of $CaMoO_4$ nanocrystalline shows the narrow central peak of the $[MoO_4]^{2-}$ excited complex at 477 nm.

Acknowledgements

We are extremely grateful to the Thailand Research Fund (TRF), and NANOTEC, a member of NSTDA, Ministry of Science and Technology, Thailand for financial support, and the Graduate School of Chiang Mai University for general funding.

References

[1] D. Chen, G. Shen, K. Tang, H. Zheng, Y. Qian, Mater. Res. Bull. 38 (2003) 1783–1789.
[2] L. Sun, M. Cao, Y. Wang, G. Sun, C. Hu, J. Cryst. Growth 289 (2006) 231–235.
[3] Z. Lou, M. Cocivera, Mater. Res. Bull. 37 (2002) 1573–1582.
[4] Y. Wang, J. Ma, J. Tao, X. Zhu, J. Zhou, Z. Zhao, L. Xie, H. Tian, Ceram. Int. 33 (2007) 693–695.
[5] J.H. Ryu, J.W. Yoon, C.S. Lim, W.C. Oh, K.B. Shim, J. Alloys Compd. 390 (2005) 245–249.
[6] T. Thongtem, A. Phuruangrat, S. Thongtem, J. Ceram. Process. Res. 9 (2008) 189–191.
[7] J.H. Ryu, B.G. Choi, J.W. Yoon, K.B. Shim, K. Machi, K. Hamada, J. Lumin. 124 (2007) 67–70.
[8] T. Thongtem, A. Phuruangrat, S. Thongtem, J. Phys. Chem. Solids 69 (2008) 1346–1349.
[9] T. Ding, J.J. Zhu, Mater. Sci. Eng. B 100 (2003) 307–313.
[10] T. Thongtem, A. Phuruangrat, S. Thongtem, Curr. Appl. Phys. 8 (2008) 189–197.
[11] J. Zhu, M. Zhou, J. Xu, X. Liao, Mater. Lett. 47 (2001) 25–29.
[12] Powder Diffract, File, JCPDS Int. Centre Diffract. Data, PA 19073-3273, USA, 2001.
[13] A. Phuruangrat, T. Thongtem, S. Thongtem, J. Ceram. Soc. Jpn. 116 (2008) 605–609.
[14] T.T. Basiev, A.A. Sobol, Y.K. Voronko, P.G. Zverev, Opt. Mater. 15 (2000) 205–216.
[15] A. Senyshyn, H. Kraus, V.B. Mikhailik, L. Vasylechko, M. Knapp, Phys. Rev. B 73 (2006) 014104-1–014104-9.
[16] D. Errandonea, J. Pellicer-Porres, F.J. Manjón, A. Segura, Ch. Ferrer-Roca, R.S. Kumar, O. Tschauner, P. Rodríguez-Hernández, J. López-Solano, S. Radescu, A. Mujica, A. Muñoz, G. Aquilanti, Phys. Rev. B 72 (2005) 174106-1–174106-14.
[17] C. Boudias, D. Monceau, CaRIne Crystallography 3.1, 17 rue du Moulin du Roy, F-60300 Senlis, France, 1989–1998.
[18] J.C. Sczancoski, L.S. Cavalcante, M.R. Joya, J.A. Varela, P.S. Pizani, E. Longo, Chem. Eng. J. 140 (2008) 632–637.
[19] S.P.S. Porto, J.F. Scott, Phys. Rev. 157 (1967) 716–719.

[20] G.M. Clark, W.P. Doyle, Spectrochim. Acta 22 (1966) 1441–1447.
[21] Z.C. Ling, H.R. Xia, D.G. Ran, F.Q. Liu, S.Q. Sun, J.D. Fan, H.J. Zhang, J.Y. Wang, L.L. Yu, Chem. Phys. Lett. 426 (2006) 85–90.
[22] J.A. Gadsden, IR Spectra of Minerals and Related Inorganic Compounds, Butterworths, 1975.
[23] J.W. Yoon, J.H. Ryu, K.B. Shim, Mater. Sci. Eng. B 127 (2006) 154–158.
[24] Y. Zhang, N.A.W. Holzwarth, R.T. Williams, Phys. Rev. B 57 (1998) 12 738–12 750.
[25] M.J. Treadaway, R.C. Powell, J. Chem. Phys. 61 (1974) 4003–4011.
[26] V. Pankratov, L. Grigorjeva, D. Millers, S. Chernov, A.S. Voloshinovskii, J. Lumin. 94–95 (2001) 427–432.